ANTIOXIDANTS & REDOX SIGNALING
Volume 14, Number 3, 2011

DOI: 10.1089/ars.2010.3284

FORUM ORIGINAL RESEARCH COMMUNICATION

High-Glucose Stimulation Increases Reactive Oxygen Species Production Through the Calcium and Mitogen-Activated Protein Kinase-Mediated Activation of Mitochondrial Fission

Tianzheng Yu,[1,*] Bong Sook Jhun,[1,2] and Yisang Yoon[1–3]

Abstract

Increased production of reactive oxygen species (ROS) from mitochondria is the main cause of hyperglycemic complications. We previously showed that hyperglycemic conditions induce mitochondrial fragmentation that is causal for ROS overproduction. This study was to identify signaling components that induce mitochondrial fragmentation in high-glucose stimulation. We found that exposing cells to the high-glucose concentration evokes increases in cytosolic Ca^{2+}. Chelating Ca^{2+} in the high-glucose medium prevented not only the Ca^{2+} transient but also mitochondrial fragmentation and the ROS increase, indicating that the Ca^{2+} influx across the plasma membrane is an upstream event governing mitochondrial fission and the ROS generation in high-glucose stimulation. We found that the high-glucose-induced Ca^{2+} increase activates the mitogen-activated protein kinase extracellular signal-regulated kinase 1/2 (ERK1/2). The Ca^{2+} chelation prevented the ERK1/2 activation, and inhibition of the ERK1/2 phosphorylation decreased mitochondrial fragmentation as well as ROS levels in high-glucose stimulation. In addition, the level of the mitochondrial fission protein dynamin-like protein 1 in mitochondria increased in high-glucose incubation in a Ca^{2+}-dependent manner. *In vitro* kinase assays showed that ERK1/2 is capable of phosphorylating dynamin-like protein 1. These results demonstrate that high-glucose stimulation induces the activation of mitochondrial fission *via* signals mediated by intracellular Ca^{2+} and ERK1/2. *Antioxid. Redox Signal*. 14, 425–437.

Introduction

Mitochondria are vital organelles of eukaryotic cells that produce cellular energy. In addition, mitochondria play important roles in cellular ion homeostasis, redox regulation, and apoptosis. Mitochondrial adenosine triphosphate production requires an electrochemical gradient across the inner mitochondrial membrane, which is generated through the proton pumping activity of the electron transport chain (ETC). Dysregulation of the ETC activity causes increased electron slippage, resulting in overproduction of toxic reactive oxygen species (ROS). The vascular and multiorgan complications in diabetes and obesity are causally associated with hyperglycemia-induced ROS overproduction (2, 6–8, 18, 36). Mitochondria are the major source of ROS in hyperglycemia, as a high concentration of glucose increases metabolic input into mitochondria, overwhelming the ETC, resulting in mitochondrial hyperpolarization and ROS overproduction (6, 33).

The cell biological aspect of mitochondria including their motility and frequent shape changes dubbed "mitochondrial dynamics" has gained much attention recently due to its association with many pathological conditions (1, 10, 13, 17, 27, 50). Mitochondria in many cell types are organized into reticular networks composed of membrane tubules. Mitochondrial shape change is mainly mediated by fission and fusion of mitochondrial tubules. Multiple proteins have been identified to participate in these processes. Most notable are the dynamin family proteins of large GTPases. The dynamin-like protein 1 (DLP1)/dynamin-related protein 1 is responsible for constriction and severing the mitochondrial tubule during the fission process (35, 37, 47). Other dynamin-related proteins mitofusin and optic atrophy 1 mediate fusion of outer and inner mitochondrial membranes, respectively (14, 15, 30).

[1]Department of Anesthesiology, University of Rochester School of Medicine and Dentistry, Rochester, New York.
[2]Mitochondrial Research and Innovation Group, University of Rochester School of Medicine and Dentistry, Rochester, New York.
[3]Department of Pharmacology and Physiology University of Rochester School of Medicine and Dentistry, Rochester, New York.
*Current affiliation: Alfaisal University College of Medicine, Riyadh, Kingdom of Saudi Arabia.

We previously found that mitochondria in cells incubated in high-glucose media undergo rapid fragmentation through the function of DLP1 (48). Importantly, inhibition of mitochondrial fission in cells exposed to hyperglycemic conditions prevented mitochondrial hyperpolarization and ROS overproduction, suggesting that mitochondrial fragmentation in hyperglycemic incubation is an early event preceding the ROS increases (48, 49). However, the signaling process that leads to mitochondrial shape change in high-glucose stimulation is not understood.

In this study, we report upstream signaling components that regulate mitochondrial morphology in high-glucose stimulation. Our experimental data indicate that the high-glucose stimulation of cells derived from the liver and cardiovascular system evokes a Ca^{2+} transient that activates the mitogen-activated protein (MAP) kinase extracellular signal-regulated kinase 1/2 (ERK1/2). Importantly, our results demonstrate that the high-glucose-induced Ca^{2+} transient and ERK1/2 activation are upstream components activating mitochondrial fission by increasing the DLP1 translocation to the mitochondria.

Materials and Methods

Cell culture conditions

The rat liver cell line Clone 9 (ATCC CRL-1439) and cardiac myoblast cell line H9c2 (ATCC CRL-1446) were maintained in Ham's F-12K and low-glucose Dulbecco's modified Eagle's medium (DMEM), respectively, supplemented with 10% fetal bovine serum (FBS), 100 U/ml penicillin, and 100 μg/ml streptomycin. Cells were incubated at 37°C, 5% CO_2. Ham's F-12K and low-glucose DMEM contain 7 and 5.56 m*M* glucose concentrations, respectively, and 35 m*M* glucose was used for high-glucose stimulation. The 35 m*M* glucose concentration was chosen for high-glucose stimulation based on more consistent elicitation of downstream effects. The stable Clone 9 cell line carrying red fluorescent protein (45) in the mitochondrial matrix was maintained in 200 μg/ml G418. Mouse aortic smooth muscle cells (SMCs) were isolated and cultured as described previously (28). Briefly, thoracic aortas were harvested from 8-week-old mice. The aortic segments were digested with collagenase and additionally with elastase/collagenase cocktail. Cells were then plated in DMEM supplemented with 10% FBS, 100 U/ml penicillin, and 100 μg/ml streptomycin. SMC lineage was confirmed by immunostaining with anti-α-actin antibodies, and cells in passages 4–6 were used for experiments. For the extracellular Ca^{2+} chelation, ethylene glycol bis(2-aminoethyl ether)-*N*,*N*,*N*′,*N*′-tetraacetic acid (EGTA) (3 m*M*) was added to the medium 15 min before the high-glucose stimulation. For transient transfection of yellow fluorescent protein (YFP)-tagged DLP, BHK-21 cells (ATCC CCL-10) were cultured in DMEM plus 10% FBS. Cells were transfected with Lipofectamin 2000 transfection reagent (Invitrogen) and used for experiments 24 h after transfection.

Calcium imaging

The intracellular Ca^{2+} change was measured using the fluorescent probe Fluo-4 (Invitrogen). Cells were loaded with 1 μM Fluo-4/AM along with 0.02% Pluronic F-127 (Invitrogen) in HEPES buffer (10 m*M* HEPES, 10 m*M* glucose, 140 m*M* NaCl, 5 m*M* KCl, 1.8 m*M* $CaCl_2$, and 2 m*M* $MgCl_2$, pH 7.4) for 30 min at 37°C and then washed three times with indicator-free HEPES buffer. Single-cell Ca^{2+} images were taken by fluorescence microscopy at room temperature. Fluorescence intensity was measured and plotted as fold changes from the initial value.

Mitochondrial morphology analyses

For morphometric analyses of mitochondria, digital images were acquired for mitochondria labeled by immunofluorescence, red fluorescent protein, or MitoTracker staining (MitoTracker Red CMX Ros; Invitrogen). The NIH-developed ImageJ software (Wayne Rasband; NIH) was used for the analysis. Digital images were processed through a convolve filter to obtain isolated and equalized fluorescent pixels (24, 48). After thresholding, individual particles (mitochondria) were subjected to the particle analysis to acquire values for circularity (4π area/perimeter^2) and lengths of major and minor axes. From these values, form factor (FF, the reciprocal of circularity value) and aspect ratio (AR, major axis/minor axis) were calculated. Both parameters have a minimal value of 1 if the particle is a small perfect circle and the values increase as it becomes longer. AR represents mitochondrial length and increases of FF indicate increases of mitochondrial complexity (length and branching) (29).

ROS measurement

The fluorescent probe dihydroethidium (DHE; Molecular Probes) was used to detect the level of ROS as reported previously (48, 49). Cells were loaded with 5 μM DHE in HEPES buffer at 37°C for 30 min. Images were acquired and fluorescence intensity was measured using IPLab imaging software (Scanalytics, Inc.).

Indirect immunofluorescence

Cells grown on the coverslip were fixed in 4% paraformaldehyde and permeabilized with 0.1% Triton X-100. After incubating in the blocking buffer containing 5% horse serum for 1 h at 37°C, cells were incubated with primary antibodies for 2 h at 37°C and then secondary antibodies for 1 h at room temperature. Antibodies used were the rabbit anti-DLP1 (46) and mouse anti-cytochrome *c* (BD Bioscience Pharmingen) for primary antibodies, and Alexa 488 or 594-conjugated antibodies (Invitrogen) for secondary antibodies. After rinsing, coverslips were mounted on glass slides with ProLong antifade reagent (Invitrogen) and cells were viewed with an Olympus IX71 epifluorescence microscope. Fluorescence images were acquired with an Evolution QEi camera (Mediacybernetics, Inc.) driven by IPLab imaging software (Scanalytics, Inc.). Acquired images were adjusted using Adobe Photoshop (Adobe Systems Inc.) software.

In vitro *kinase assay*

Both recombinant DLP1 purified from bacteria and YFP-DLP1 immunoisolated from transfected cells were used for the *in vitro* kinase assay with ERK1. Full-length DLP1 tagged with 6×histidine (6xHis-DLP1) was expressed and purified from *Escherichia coli* using ProBond resin (Invitrogen) as

described before (47). Anti-DLP1 antibodies (46) and Protein A-agarose (Thermo Scientific) were used for immunoprecipitation from BHK-21 cells transfected with YFP-DLP1. *In vitro* kinase assays for ERK1 activity were performed by incubation of 0.2 μg of ERK1 kinase (Cell Signaling Technology) with 0.5 μg of purified 6xHis-DLP1 in 20 μl kinase assay buffer (5 m*M* MOPS [pH 7.2], 5 m*M* $MgCl_2$, 2.5 m*M* β-glycerophosphate, 1 m*M* EGTA, 0.4 m*M* EDTA, 50 μ*M* DTT, and 100 μ*M* adenosine triphosphate) at 30°C for 1 h. For immunoprecipitated DLP1, the immune complex was treated with alkaline phosphatase (Roche Applied Science) for 1 h at 37°C and then equilibrated with the kinase assay buffer before the addition of ERK1. The reaction was stopped by adding sodium dodecyl sulfate sample buffer and boiling. The samples were resolved by sodium dodecyl sulfate–polyacrylamide gel electrophoresis and then subjected to immunoblot analyses with anti-phospho-MAP kinase substrate antibody (Cell signaling Technology).

Results

High-glucose stimulation evokes the intracellular Ca^{2+} transient

Our previous results demonstrated that high-glucose stimulation increases the accumulation of short and fragmented mitochondria, which is an upstream event in hyperglycemia-mediated ROS overproduction and cell injury in cells from the liver and cardiovascular system (48, 49). We also found that the inhibition of pyruvate transport from the cytosol to the mitochondrial matrix during hyperglycemic stimulation prevented the ROS increase, but mitochondrial fragmentation still persisted upon the pyruvate transport blockage (48). This result suggests that a cytosolic signal generated between the glucose uptake and pyruvate production is responsible for the high-glucose-induced mitochondrial fragmentation. In pancreatic β-cells, high-glucose stimulation induces a cytosolic Ca^{2+} increase (20, 23, 38, 42). In addition, we and others have reported that increasing intracellular Ca^{2+} levels induced mitochondrial fragmentation, indicating that Ca^{2+} is one of the factors that regulate mitochondrial morphology (24, 39). Therefore, we first tested whether Ca^{2+} participates in regulating mitochondrial morphology in high-glucose stimulation. Using Clone 9 rat liver cells, Ca^{2+} imaging experiments showed a rapid increase and subsequent decrease of cytosolic Ca^{2+} upon incubation in the high-glucose concentration (Fig. 1A). The Ca^{2+} level increased immediately after increasing the glucose concentration to 35 m*M*, and returned to the basal level in 5–10 min. This Ca^{2+} increase is faster than mitochondrial fragmentation and ROS increase (48), suggesting that increased cytosolic Ca^{2+} may be an early signal for mitochondrial fragmentation in high-glucose conditions. Adding the same concentration of the stereoisomer L-glucose in the place of D-glucose did not increase cytosolic Ca^{2+}. These data demonstrate that glucose metabolism is necessary for the intracellular Ca^{2+} increase much like for the mitochondrial fragmentation and ROS increase (48).

Cell stimulations often evoke cytosolic Ca^{2+} through Ca^{2+} entry from the extracellular medium. To test whether extracellular Ca^{2+} plays a role in the high-glucose-induced intracellular Ca^{2+} increase, we depleted extracellular Ca^{2+} during high-glucose stimulation. As shown in Figure 1B,

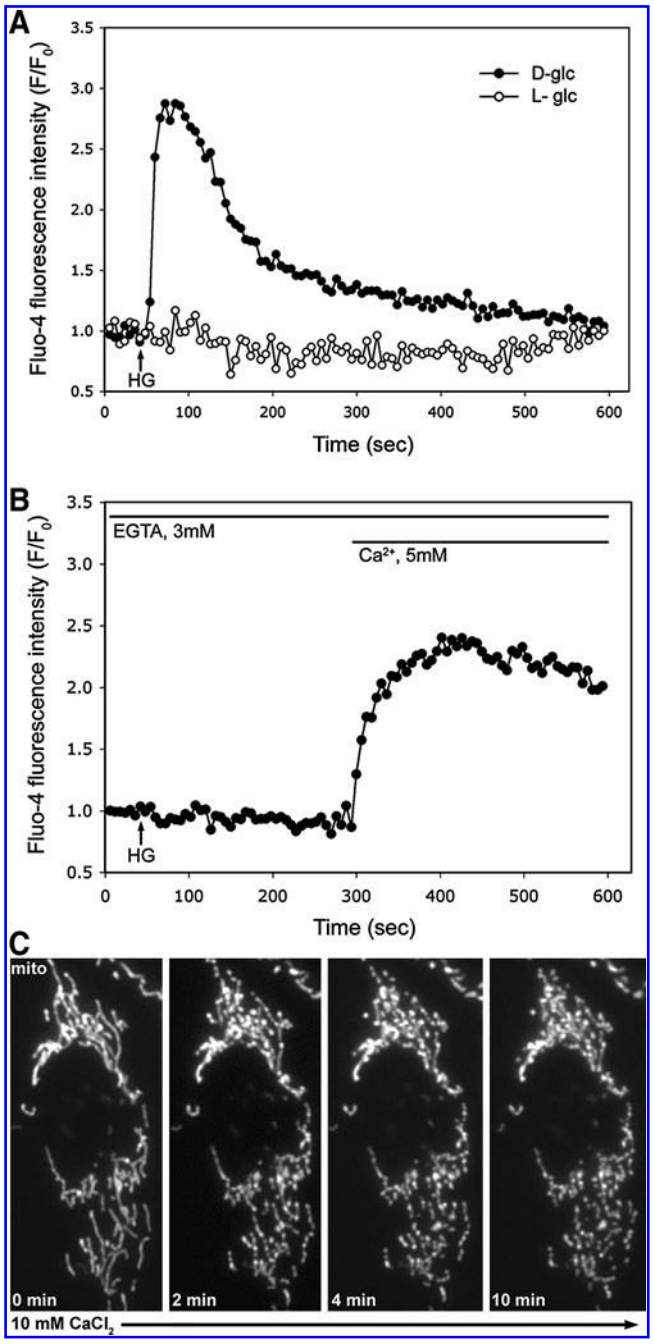

FIG. 1. High-glucose incubation evokes Ca^{2+} transient through the Ca^{2+} influx that induces mitochondrial fragmentation. (**A**) Ca^{2+} imaging using Fluo-4 shows cytosolic Ca^{2+} increase in high-glucose stimulation of Clone 9 cells. The Ca^{2+} increase was transient as it decreases to the resting level in 5–10 min. The stereoisomer L-glucose did not evoke the Ca^{2+} transient. (**B**) Chelating the extracellular Ca^{2+} by adding ethylene glycol bis(2-aminoethyl ether)-*N*,*N*,*N*′,*N*′-tetraacetic acid (EGTA) (3 m*M*) to the medium abolished the Ca^{2+} transient upon the high-glucose stimulation. Addition of excess Ca^{2+} in the presence of EGTA increased the cytosolic Ca^{2+}. (**C**) Increasing the extracellular Ca^{2+} concentration induced mitochondrial fragmentation. Ca^{2+} was added to 10 m*M* to the culture medium of Clone 9 cells carrying red fluorescent protein in mitochondria, and time-lapse imaging was performed. Mitochondrial fragmentation is evident in 2 min of the Ca^{2+} addition.

3 m*M* EGTA in the extracellular medium abolished the cytosolic Ca^{2+} transient upon high-glucose stimulation. Readdition of excess Ca^{2+} to the extracellular medium increased the cytosolic Ca^{2+} (Fig. 1B). These results demonstrate that extracellular Ca^{2+} is necessary for the high-glucose-induced Ca^{2+} transient.

The high-glucose-induced Ca^{2+} increase is necessary for mitochondrial fragmentation

Because we found that extracellular Ca^{2+} is an important factor for evoking the high-glucose-induced Ca^{2+} increase (Fig. 1B), we tested the role of Ca^{2+} in mitochondrial morphology in normal and high-glucose conditions. Initially, we simply increased the extracellular Ca^{2+} concentration and examined mitochondrial morphology. Upon increasing the Ca^{2+} concentration to 10 m*M*, time-lapse imaging showed a clear change in mitochondrial morphology (Fig. 1C). Mitochondrial tubules converted to nodular and beads-on-the-string morphology within 2 min, and many of them formed discrete small mitochondria, indicating that increasing the extracellular Ca^{2+} concentration caused mitochondrial fragmentation. Because extracellular Ca^{2+} is necessary for the high-glucose-induced Ca^{2+} increase, we next examined mitochondrial morphology in Clone 9 cells bathed in the EGTA-containing medium with or without high-glucose stimulation. In the absence of EGTA, tubular mitochondria became fragmented upon high-glucose stimulation as shown before (48) (Fig. 2C). With EGTA in the extracellular medium under normal glucose conditions, we observed that mitochondria were tubular (Fig. 2B). These mitochondria were often more elongated (Fig. 2B), suggesting that chelating extracellular Ca^{2+} may decrease the normal fission process. We found that upon high-glucose stimulation in the presence of EGTA, cells still maintained tubular mitochondrial morphology (Fig. 2D). Morphometric analyses of individual mitochondria were performed for objective evaluation of mitochondrial morphology. We calculated the AR and FF that reflect tubule length as well as branching (24, 29, 48). The minimal values of both FF and AR are 1, representing a perfect circle, with the values increasing as the shape elongates and branches. As depicted in scatter charts (Fig. 2E), most of the mitochondria in high-glucose incubation are crowded close to the minimum value for FF and AR, indicating mitochondrial fragmentation. The addition of EGTA increased the FF and AR, indicative of mitochondrial elongation (Fig. 2E).

We also observed the same effect of EGTA on mitochondrial morphology in aortic SMCs and the cardiac myoblast cell line H9c2. Similar to the observation made in Clone 9 cells, both cell types from the cardiovascular system showed the high-glucose-induced mitochondrial fragmentation that is attenuated by EGTA (Fig. 3A, B). Cell counting at different time points of the high-glucose stimulation demonstrated that the high-glucose-mediated mitochondrial fragmentation was transient during the first hour as reported before (48), and EGTA abolished this phenomenon (Fig. 3C), indicating that the Ca^{2+} influx across the plasma membrane is required for mitochondrial fragmentation in high-glucose stimulation. This series of results supports our notion that the Ca^{2+} transient evoked from high-glucose exposure acts as an upstream signal that regulates mitochondrial morphology.

Ca^{2+} increase is necessary for ROS overproduction in high-glucose conditions

Because the Ca^{2+} increase was required for mitochondrial fragmentation (Fig. 2) that acts as an upstream factor for the ROS increase in high-glucose conditions (48, 49), we tested whether the Ca^{2+} increase is necessary for the ROS increase in high-glucose stimulation. To this end, we incubated cells in the Ca^{2+}-free media and measured ROS levels in high-glucose stimulation. ROS levels were measured using the fluorescent probe DHE, which is oxidized by superoxide anion and produces ethidium that binds to DNA in the nucleus. As shown in Figure 4, the high-glucose incubation increased nuclear ethidium fluorescence due to the ROS overproduction in Ca^{2+}-containing media (Fig. 4C, E). The ROS increase is likely the mitochondrial origin as decreasing the mitochondrial membrane potential or inhibiting mitochondrial pyruvate transport abolished the ROS increase in high-glucose stimulation (48). In the presence of EGTA, however, ROS levels remained low despite high-glucose conditions (Fig. 4D, E). These results indicate that the Ca^{2+} increase induced in high-glucose stimulation is an upstream component for the ROS increase.

High-glucose stimulation activates the MAP kinase ERK1/2 through the Ca^{2+} increase

Glucose stimulation of pancreatic β-cells has been shown to activate the MAP kinase ERK1/2 through Ca^{2+} signaling (3, 20, 26). Therefore, we next tested the role of ERK1/2 in high-glucose-induced mitochondrial fragmentation and ROS increase in our experimental system. Immunoblotting with phospho-specific ERK1/2 antibodies indicated that ERK1/2 in aortic SMCs became rapidly phosphorylated in 5 min of high-glucose exposure (35 m*M*) (Fig. 5A). Pronounced ERK1/2 phosphorylation was observed in 5- and 15-min incubations, and it decreased in 30 and 60 min in high-glucose incubation (Fig. 5A). We also tested ERK1/2 phosphorylation in Clone 9 cells and found a similar trend of a transient ERK1/2 phosphorylation (Fig. 5B). This temporal profile of ERK1/2 phosphorylation is comparable to those of mitochondrial morphology and ROS levels in high-glucose exposure (48), suggesting that the ERK1/2 signaling plays a role in the mitochondrial morphology change and ROS increase upon high-glucose stimulation. To test whether the ERK1/2 activation in high-glucose incubation is Ca^{2+} dependent, we preincubated cells with EGTA. We found that EGTA abolished the ERK1/2 activation in high-glucose stimulation (Fig. 5C), indicating that the Ca^{2+} increase is the upstream factor for the high-glucose-induced ERK1/2 activation.

Inhibition of the ERK1/2 activation decreases mitochondrial fragmentation and prevents the ROS increase in high-glucose stimulation

Our results demonstrated that high-glucose stimulation rapidly increases cytosolic Ca^{2+}, which induces mitochondrial fragmentation, ROS increase, and the ERK1/2 activation. Our previous studies have shown that mitochondrial fragmentation is causal for the ROS increase in high-glucose stimulation (48, 49). To further delineate the role of ERK1/2 activation in mitochondrial fragmentation and the ROS increase, we specifically inhibited the ERK1/2 phosphorylation

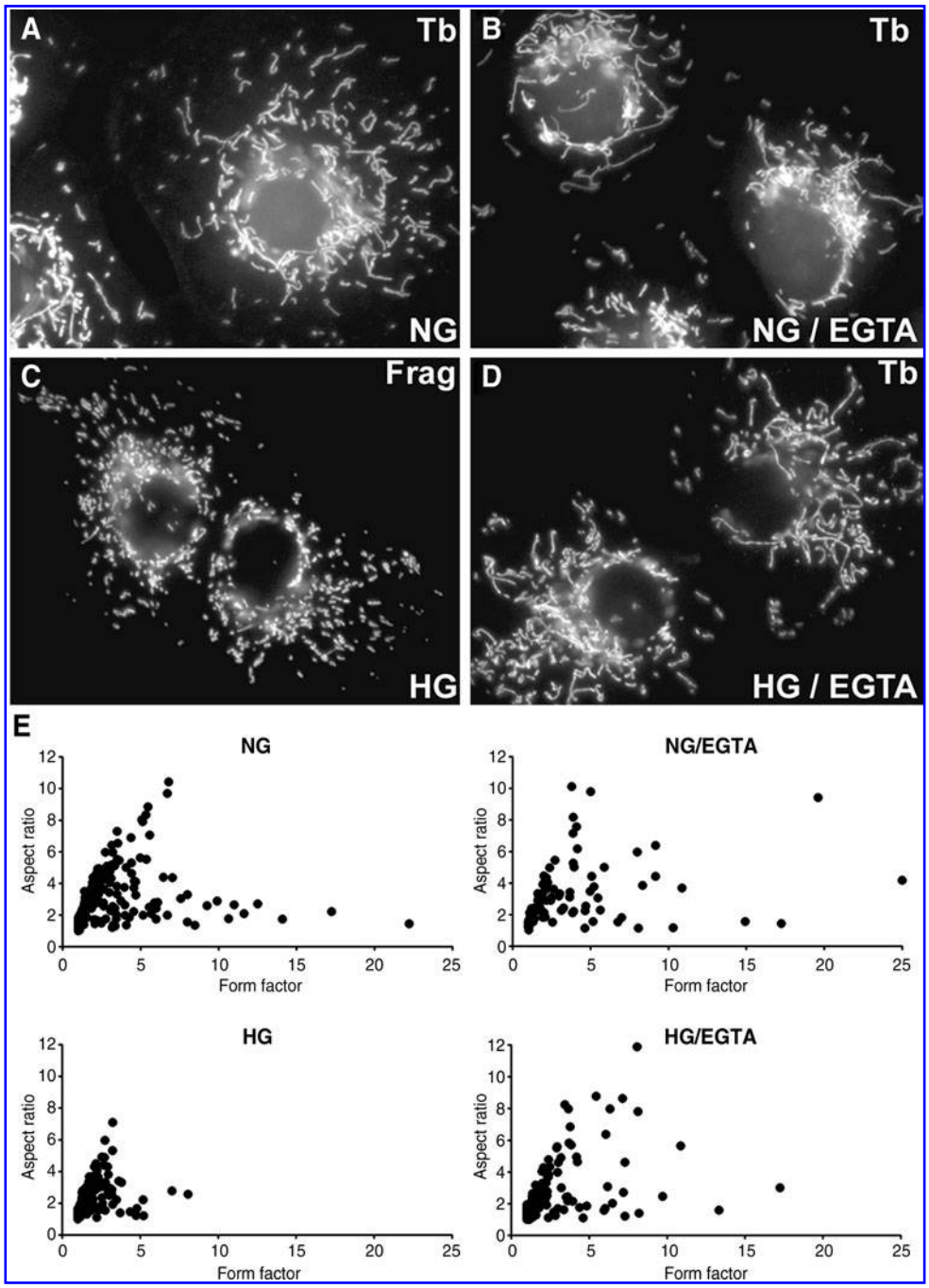

FIG. 2. Ca^{2+} chelation inhibits the high-glucose-induced mitochondrial fragmentation. Clone 9 cells harboring RFP-labeled mitochondria were incubated with (**B** and **D**) and without (**A** and **C**) 3 m*M* EGTA in the culture medium. Mitochondrial morphology was assessed after 15-min incubation in the 35 m*M* glucose. NG, normal glucose concentration, HG, high-glucose concentration, Tb, tubular, Frag, fragmented. (**E**) The computer-assisted morphometric analyses of mitochondrial morphology. Mitochondria in cells incubated in the high-glucose concentration (HG) show lower values of form factor and aspect ratio. Mitochondria of cells in high-glucose medium along with EGTA (HG/EGTA) display many mitochondria with higher values of FF and AR, indicating long and branched mitochondria.

using the MAP/ERK kinase 1 inhibitor PD98095, and examined mitochondrial morphology and the ROS levels upon high-glucose exposure. With preincubating cells with PD98059 before the high-glucose exposure, we found that tubular mitochondria are maintained in high-glucose conditions. While mitochondrial fragmentation was evident at 15- and 30-min incubations in high-glucose media, the PD98059 treatment significantly decreased the fragmentation effect of high-glucose stimulation (Fig. 6). It was often noticed that mitochondria in cells treated with PD98059 and high glucose were less tubular and showed more pronounced perinuclear condensation. Morphometric analyses of mitochondrial morphology demonstrated that the inhibition of ERK1/2 phosphorylation decreased high-glucose-induced mitochondrial fragmentation, as values of both FF and AR of many mitochondria remained high with PD98059 in high-glucose incubation (Fig. 6). An inhibitor of the Ca^{2+}/calmodulin-dependent protein kinase II, KN-93, had no effect on mitochondrial morphology in high-glucose stimulation, mirroring the same time frame of mitochondrial fragmentation as observed with the high-glucose treatment alone (Fig. 6). These results indicate an ERK1/2-specificity for the high-glucose-mediated change of mitochondrial morphology. Cell counting determined that, in the presence of PD98059, 35%–45% of high-glucose-exposed cells had fragmented mitochondria, whereas ~80% of them exhibited mitochondrial fragmentation in the

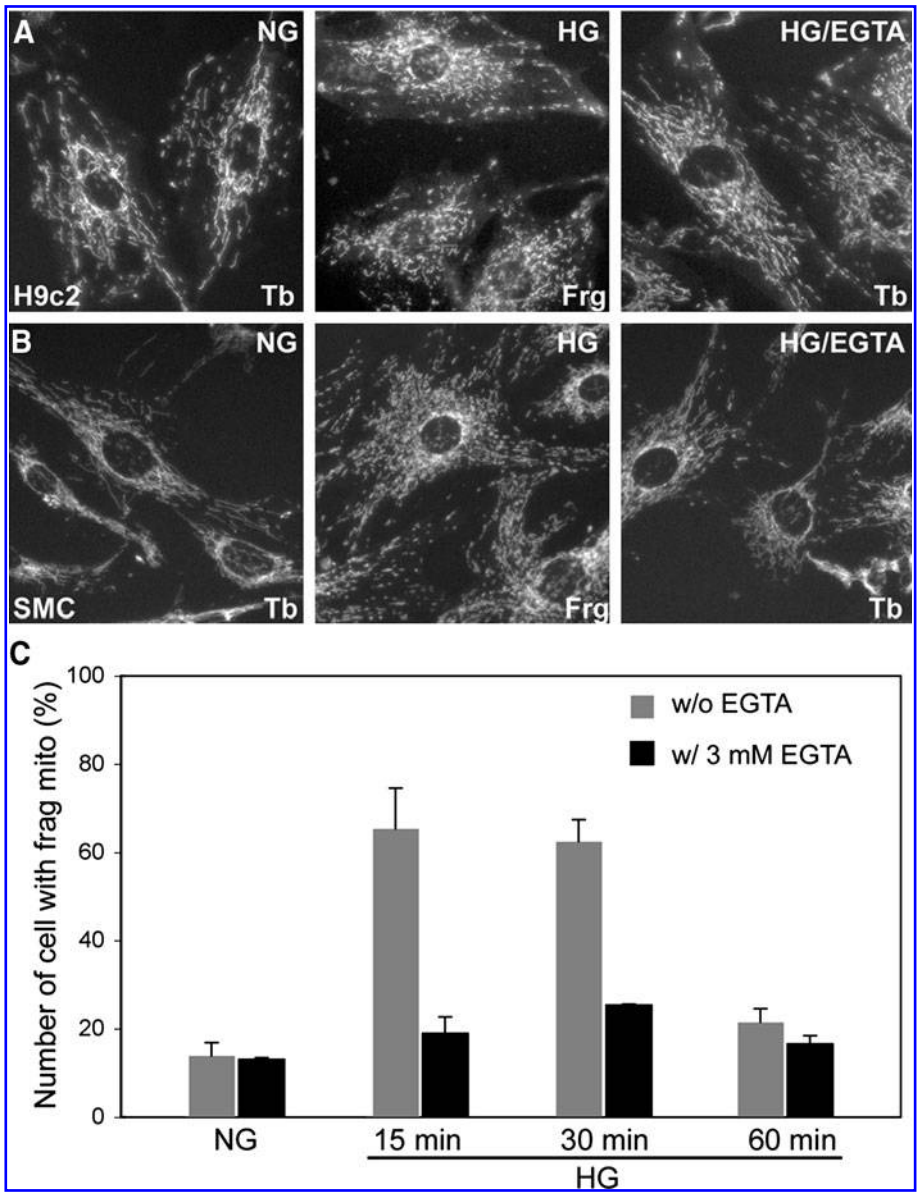

FIG. 3. EGTA inhibits the high-glucose-induced mitochondrial fragmentation in cells derived from the cardiovascular system. The cardiac myoblast cell line H9c2 (**A**) and aortic smooth muscle cells (SMC, **B**) were subjected to high-glucose stimulation with and without extracellular EGTA. Mitochondria were labeled with anti-cytochrome *c* antibodies. Mitochondria of cells in high-glucose medium (15 min) were fragmented, and EGTA decreased the fragmentation effect of the high-glucose medium. (**C**) Cell counting of H9c2 cells during the time course of high-glucose incubation. EGTA abolished the high-glucose-induced transient fragmentation of mitochondria.

absence of the inhibitor (Fig. 7A), indicating a significant role of the ERK1/2 activation in the high-glucose-induced mitochondrial fragmentation. No significant effect was found with KN-93 (Fig. 7A).

Under the same experimental conditions, ROS measurements showed that PD98095 prevented the ROS increase upon the high-glucose exposure (Fig. 7B), indicating that the ERK1/2 activation is necessary for the high-glucose-induced ROS increase. KN-93 had no effect on ROS level in high-glucose stimulation (Fig. 7B), suggesting a specific role of ERK1/2 phosphorylation in high-glucose-mediated ROS overproduction. These experimental data demonstrated that ERK1/2 phosphorylation is an upstream factor causing mitochondrial fragmentation and ROS increase upon high-glucose stimulation. Based on our current and previous results, the upstream signaling sequence leading to the ROS overproduction in high-glucose stimulation is likely in the order of Ca^{2+}, ERK1/2, and mitochondrial fission (Fig. 7C).

The high-glucose-mediated Ca^{2+} increase induces the DLP1 translocation to mitochondria

We have shown that inhibition of mitochondrial fission blocks mitochondrial fragmentation and ROS increase in high-glucose exposure (48, 49). Because our data indicate that the high-glucose-induced cytosolic Ca^{2+} increase and the ERK1/2 activation are the upstream signals for mitochondrial fragmentation, we hypothesized that the Ca^{2+}-induced ERK1/2 phosphorylation activates mitochondrial fission in high-glucose stimulation of cells. The DLP1 is a cytosolic mechanochemical enzyme that translocates to the mitochondrial surface for the fission reaction. It has been shown that the level of DLP1 associated with the mitochondria increases during fission-activating conditions such as apoptosis (5, 21). To test whether DLP1 subcellular distribution changes during high-glucose stimulation, we performed immunofluorescence microscopy of DLP1. In resting normal glucose conditions, most DLP1 distributes to the cytosol with a subpopulation

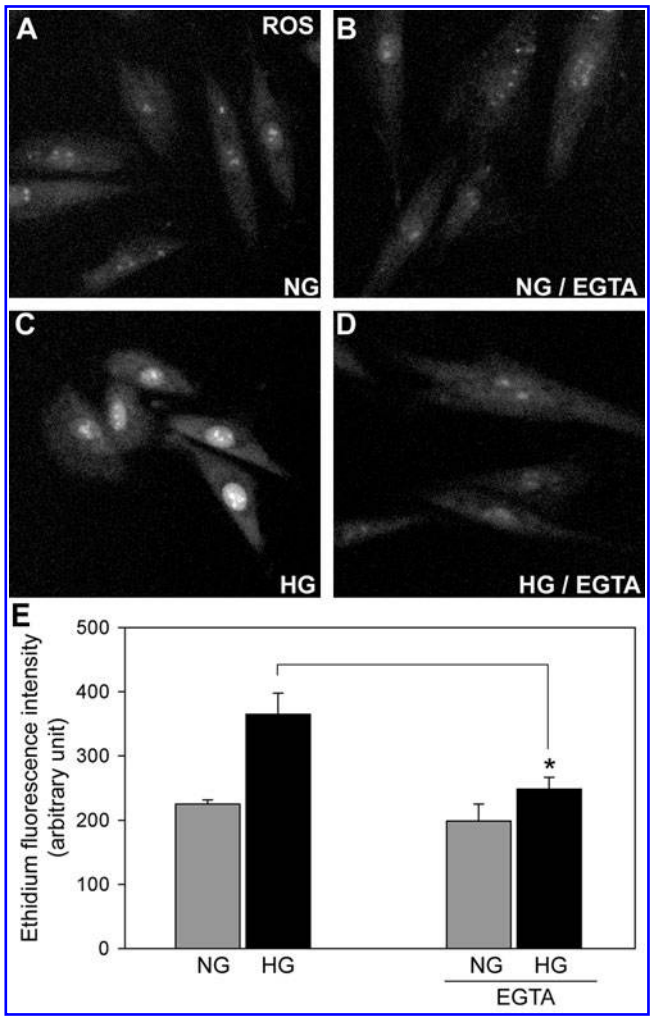

FIG. 4. Extracellular Ca^{2+} is necessary for the reactive oxygen species (ROS) increase in high-glucose conditions. H9c2 cells incubated in the presence (**B** and **D**) and absence (**A** and **C**) of EGTA were subjected to the high-glucose stimulation. High-glucose conditions increased the ROS levels, as assessed by dihydroethidium (**C**). Cells preincubated with EGTA did not increase ROS levels in high-glucose conditions (**D**). (**E**) ROS levels were quantified by the ethidium fluorescence intensity. ROS measurements were performed at 15 min in high-glucose incubation. Error bars represent SEM. $*p < 0.05$.

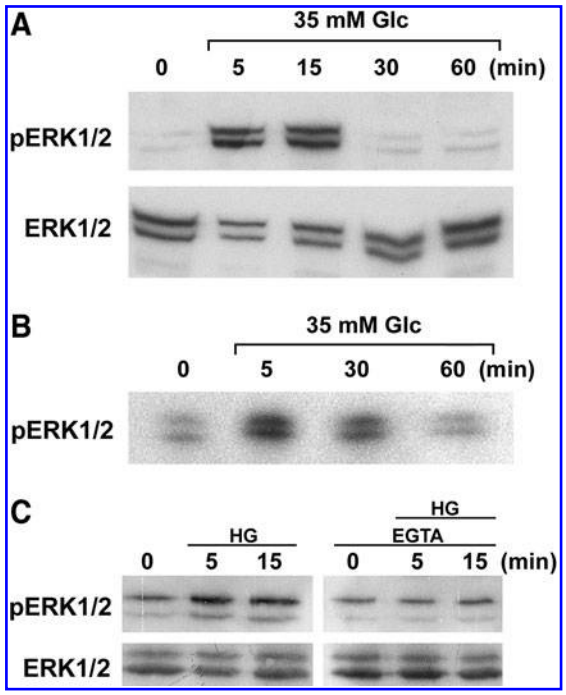

FIG. 5. High-glucose incubation activates extracellular signal-regulated kinase 1/2 (ERK1/2) in a Ca^{2+}-dependent manner. Cell lysate was prepared at indicated times of high-glucose incubation, and the ERK1/2 activation was assessed by immunoblotting. Phospho-ERK1/2-specific antibodies detected the activation of ERK1/2 in SMC (**A**), Clone 9 (**B**), and H9c2 cells (**C**). Immunoblotting with antibodies recognizing total ERK1/2 showed the relatively equal loading. (**C**) EGTA preincubation abolished the ERK1/2 activation in high-glucose conditions.

associated with mitochondrial tubules as punctate spots (Fig. 8A). Cells in the EGTA-containing normal glucose medium had elongated mitochondria and more diffuse cytosolic DLP1 (Fig. 8C). In contrast, cells incubated in the high-glucose concentration revealed that DLP1 in the cytoplasm formed more pronounced foci, and more DLP1 puncta were associated with small fragmented mitochondria (Fig. 8B). The inclusion of EGTA in the high-glucose medium abolished the mitochondrial fragmentation. In addition, cytoplasmic DLP1 was more diffuse similar to the distribution in normal glucose conditions (Fig. 8D). We also isolated mitochondrial fractions from cells exposed to normal and high-glucose concentrations and assessed the DLP1 levels. Immunoblot analyses indicate that the mitochondrial fraction isolated from cells incubated in high glucose contained an increased level of DLP1, compared to that from cells incubated with the normal glucose concentration (Fig. 8E). Preincubating cells with EGTA decreased DLP1 levels in the mitochondrial fraction in both normal and high-glucose conditions (Fig. 8E), suggesting that Ca^{2+} plays a role in DLP1 translocation during normal fission as well as high-glucose-induced mitochondrial fission.

Our results demonstrated that the high-glucose stimulation evokes intracellular Ca^{2+} transient and activates ERK1/2. In turn, this increases mitochondrial fission through the DLP1 function, raising the possibility that DLP1 may be a substrate for ERK1/2. To test whether ERK1/2 directly phosphorylates DLP1, we performed *in vitro* kinase assay using active ERK1 and recombinant DLP1. Our data demonstrate that ERK1 is capable of phosphorylating DLP1 (Fig. 8F). Using the antibody recognizing phosphorylated MAP kinase substrates, phosphorylated DLP1 was detected in the presence of the active ERK1, but not in the absence of the kinase. ERK1 also phosphorylated DLP1 isolated from cells (Fig. 8G). Cells transfected with DLP1 fused to YFP (YFP-DLP1) were subjected to immunoprecipitation with anti-DLP1 antibodies. A significant amount of YFP-DLP1 was phosphorylated in cells, as the anti-phospho MAP kinase substrate antibody reacted with the immunoprecipitated protein and the phosphatase treatment abolished the antibody reactivity (Fig. 8G). Phosphorylation of immunoprecipitated endogenous DLP1 was barely detectable. The subsequent addition of ERK1 to the

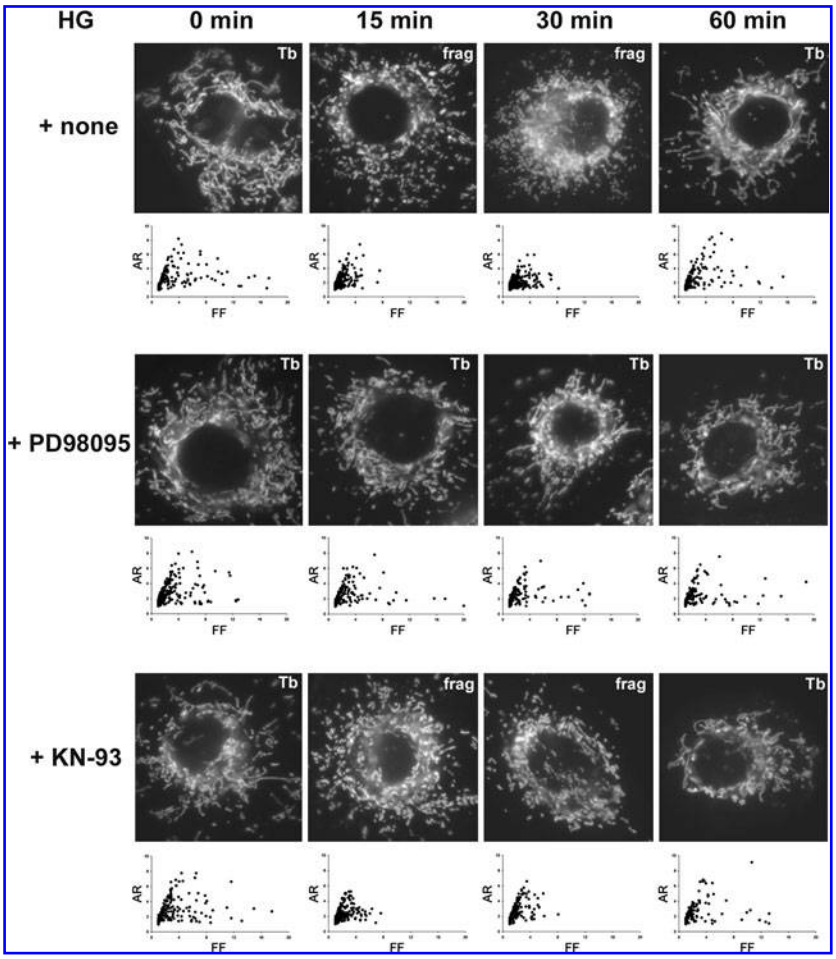

FIG. 6. Inhibition of the ERK1/2 activation prevents the high-glucose-induced mitochondrial fragmentation. The mitogen-activated protein/ERK kinase 1 inhibitor PD98095 that blocks the ERK1/2 phosphorylation decreased the mitochondrial fragmentation in high-glucose incubation. Treating with KN-93 that inhibits Ca^{2+}/calmodulin-dependent kinase II showed no effect on the high-glucose-induced mitochondrial fragmentation. Morphometric analyses indicate that tubular mitochondria were maintained throughout the high-glucose stimulation in the presence of PD98095.

phosphatase-treated material phosphorylated DLP1 (Fig. 8G). We located the serine residue (S616) in the C-terminal region of DLP1 as a potential ERK1/2 phosphorylation site through sequence analyses (Fig. 9A), and tested whether the S616 is the site phosphorylated by ERK1. The *in vitro* kinase assay using both wild type and the serine-to-alanine mutant (S616A) of DLP1 demonstrated that the S616A mutation abolished the ERK1-mediated DLP1 phosphorylation (Fig. 8H). These data indicate that DLP1 can be phosphorylated at the S616 by ERK1/2. Taken together, results presented in this study indicate that high-glucose stimulation induces the Ca^{2+}-mediated MAP kinase signaling that increases mitochondrial fission and ROS levels possibly through the ERK1/2-dependent DLP1 phosphorylation.

Discussion

ROS overproduction from mitochondria contributes to oxidative stress-induced cell injury, leading to hyperglycemic complications in diabetes. Our previous studies demonstrated that mitochondrial fission is an upstream causal factor for ROS increase during hyperglycemic insult and that inhibiting mitochondrial fragmentation in high-glucose incubation normalizes ROS levels and decreases apoptosis (48, 49). This study is to identify high-glucose-mediated signaling mechanisms that govern the mitochondrial fission process and subsequently the ROS increase.

We identified Ca^{2+} as an early signaling factor for mitochondrial fragmentation in the high-glucose stimulation (Figs. 1 and 2). Ca^{2+} is a versatile signaling component that participates in the multitude of intracellular signaling pathways (4). With respect to mitochondrial morphology, we have shown that the thapsigargin-mediated Ca^{2+} increase fragments mitochondria (24). Therefore, it is not surprising that Ca^{2+} is also involved in the high-glucose-induced mitochondrial fission. It is not known how high-glucose concentration increases the intracellular Ca^{2+}. L-glucose did not evoke the Ca^{2+} transient, indicating that glucose metabolism is necessary for the Ca^{2+} increase (Fig. 1). Our previous results revealed that inhibiting pyruvate transport from the cytosol to mitochondria still results in fragmented mitochondria in high-glucose stimulation (48), suggesting the involvement of a cytosolic process, possibly glycolysis, in high-glucose-induced mitochondrial fission (Fig. 9B). The Ca^{2+} transient occurs within minutes of glucose stimulation (Fig. 1). Glycolysis is a rapid cytosolic process. Therefore, it will be interesting to test whether certain glycolytic intermediates play a role in the high-glucose-induced Ca^{2+} increase. We also found that the Ca^{2+} entry across the plasma membrane is required for the intracellular Ca^{2+} increase upon the glucose stimulation (Fig. 1). The glycolytic complex is presumed to be in proximity to the both plasma membrane and mitochondria for rapid conversion of glucose and efficient channeling of pyruvate to mitochondria, as evidenced by the association of the

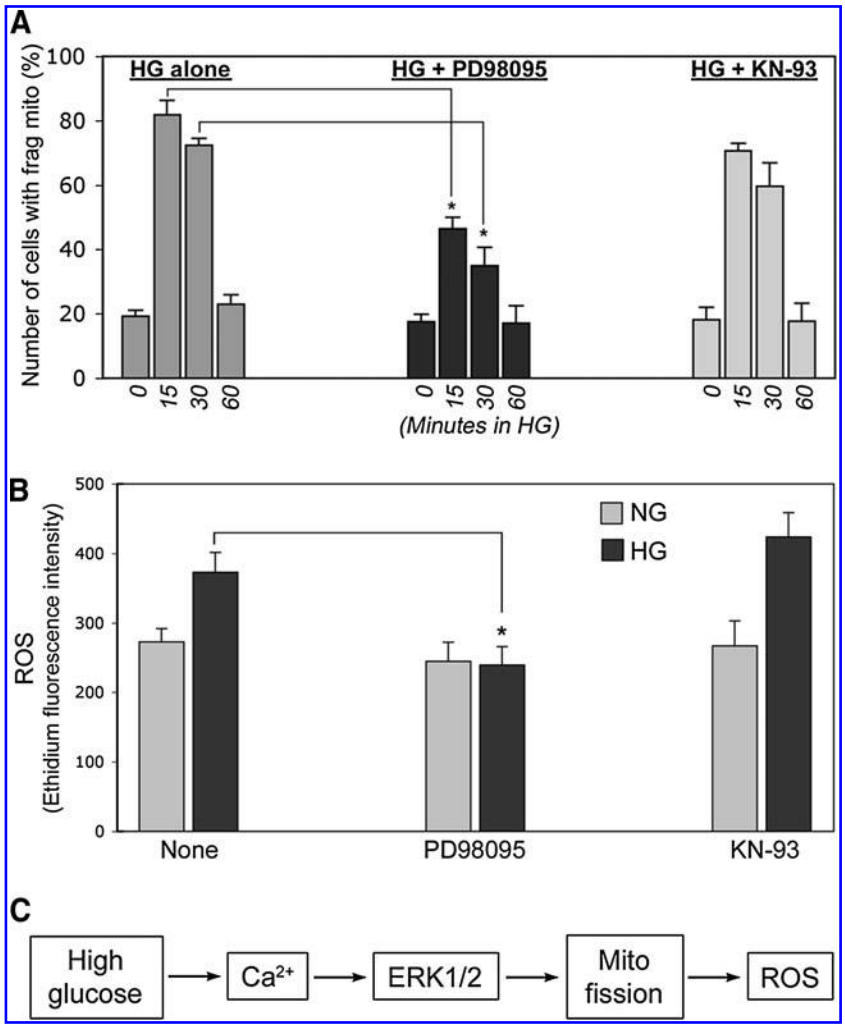

FIG. 7. The high-glucose-induced Ca^{2+} increase and ERK1/2 activation lead to mitochondrial fragmentation and the ROS increase. (**A**) Cell counting revealing a reduction of the high-glucose-induced mitochondrial fragmentation upon inhibition of the ERK1/2 activation. Error bars represent SEM. $*p < 0.05$. (**B**) ROS, assessed by dihydroethidium fluorescence, in H9c2 cells demonstrated that PD98059, but not KN-93, decreased the high-glucose-induced ROS increase, indicating the necessary role of the ERK1/2 activation in this process. ROS was measured at 15 min in high-glucose incubation (HG). NG, normal glucose incubation. Error bars represent SEM. $*p < 0.05$. (**C**) The sequence of events leading to the ROS increase in high-glucose stimulation.

glycolytic enzyme hexokinase with the mitochondrial outer membrane (19, 31, 34, 43). Therefore, it is possible that there is a physical connection between glycolysis and the plasma membrane Ca^{2+} entry channel through which increased glucose uptake and glycolysis activate Ca^{2+} influx. It is currently unclear whether the acute high-glucose stimulation evokes the capacitative Ca^{2+} entry. It was reported that hyperglycemia-induced apoptosis requires the store-operated Ca^{2+} entry during prolonged high-glucose conditions in endothelial cells (41). Further studies will elucidate how intracellular Ca^{2+} stores and additional signaling components take part in controlling mitochondrial fission in high-glucose stimulation.

It is interesting that mitochondria in cells incubated in the Ca^{2+}-free medium appear more elongated than those in normal medium conditions. This observation suggests that Ca^{2+} is necessary for mitochondrial fission in normal resting condition as well. High-glucose stimulation as well as other Ca^{2+}-evoking conditions such as thapsigargin or Ca^{2+} ionophore treatment would amplify the Ca^{2+} signal, promoting increased mitochondrial fission and fragment mitochondria.

Activation of the MAP kinase ERK1/2 has been identified to be a major signaling event occurring upon glucose stimulation in the pancreatic β-cell line (3, 20, 26). The ERK1/2 activation in β-cells depends on glucose metabolism and subsequent increase of cytosolic Ca^{2+} (3, 20). In our study with cells derived from the liver and cardiovascular system, we have also detected the ERK1/2 activation following the high-glucose stimulation and Ca^{2+} increase, indicating that glucose-mediated ERK1/2 activation is a common early signaling event in variety of cell types. While the downstream effect of ERK1/2 in β-cells is largely associated with transcriptional regulation, we identified the ERK1/2 activation as a high-glucose-induced signaling that enhances mitochondrial fission. Our data raise an intriguing possibility that DLP1 is a direct substrate phosphorylated by ERK1/2 (Fig. 8F–H). Thus far, three different kinases have been reported to phosphorylate DLP1. A phosphorylation of DLP1 at the C-terminal coiled coil region by cyclic adenosine monophosphate-dependent protein kinase decreases mitochondrial fission (11, 16), whereas the phosphorylation at the same serine residue (S637) by calmodulin-dependent kinase Iα enhances fission (22) (Fig. 9A). Another phosphorylation at the different serine residue (S616) of DLP1 by the cyclin-dependent kinase (CDK1) during mitosis activates mitochondrial fission (40). The amino acid sequence surrounding the CDK1 phosphorylation site (-MPASPQKG-) contains the ERK1/2 phosphorylation consensus PXSP, suggesting that ERK1/2 may phosphorylate DLP1 at the same serine residue

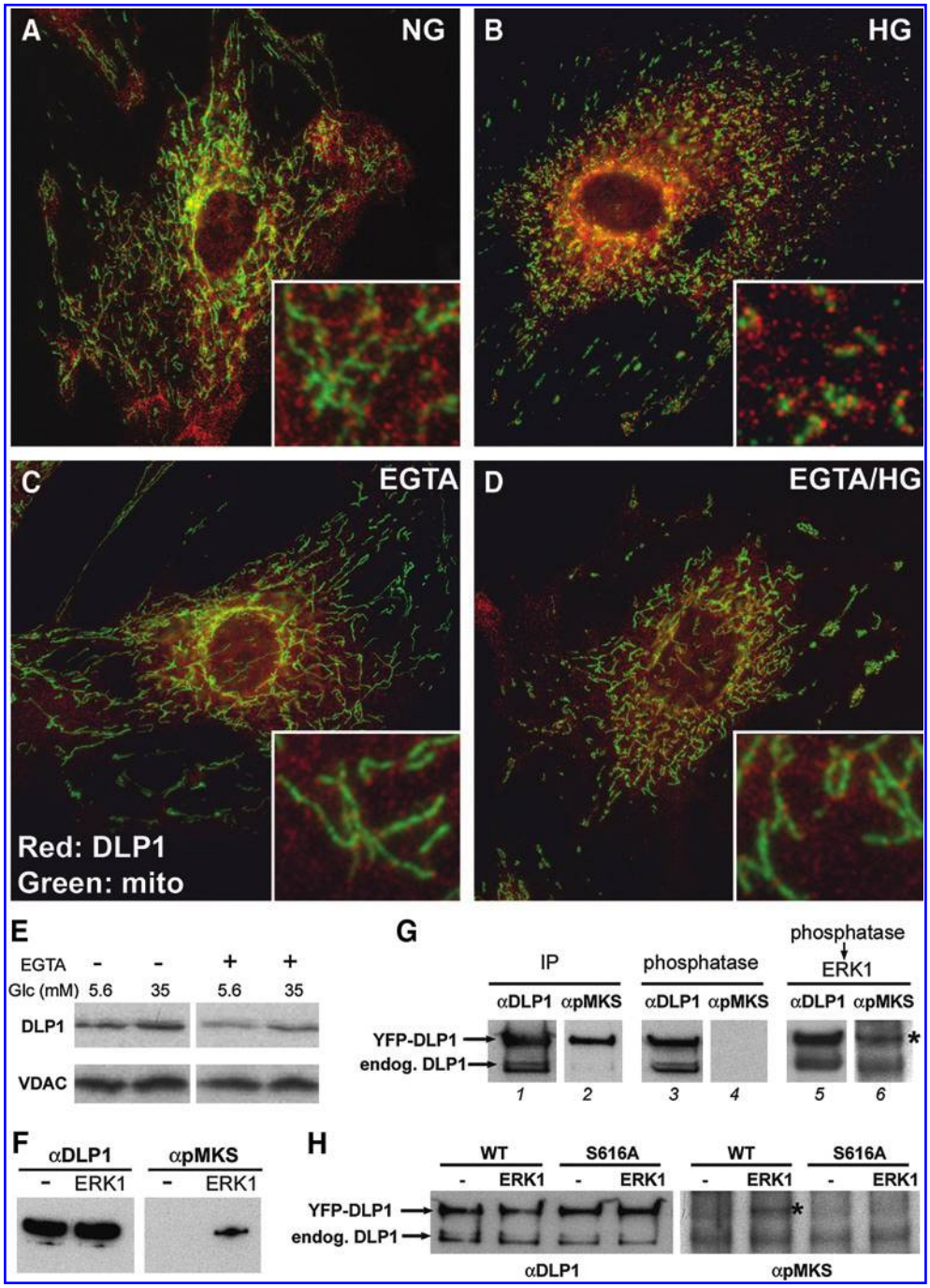

FIG. 8. High-glucose-induced mitochondrial fragmentation is mediated by dynamin-like protein 1 (DLP1) function. (**A–D**) Immunofluorescence staining for DLP1 (red) and mitochondria (green) in SMC following a 15-min incubation in high-glucose conditions with or without EGTA. Insets are fivefold magnified image of a part of the whole cell image. DLP1 is mostly cytosolic in normal glucose (**A**). In high-glucose stimulation, DLP1 forms localized foci, many of which are associated with small fragmented mitochondria (**B**). EGTA abolished the foci-forming effect of the high-glucose stimulation (**D**). (**E**) Immunoblotting for DLP1 in the mitochondrial fraction isolated from normal and high-glucose conditions with and without EGTA. High-glucose stimulation increased the DLP1 level associated with mitochondria while EGTA preincubation decreased it. Anti-voltage-dependent anion channel (VDAC) antibodies were used for loading control. (**F–H**) *In vitro* phosphorylation of DLP1 by ERK1. Purified recombinant DLP1 was incubated with or without active ERK1 and DLP1 phosphorylation was detected by anti-phospho-mitogen-activated protein kinase substrate antibodies (αpMKS) (**F**). (**G**) Yellow fluorescent protein (YFP)-DLP1 was isolated from transfected cells by immunoprecipitation (IP). While the anti-DLP1 antibodies show both YFP-DLP1 and endogenous DLP1 in the IP sample (*lanes 1, 3, and 5*), immunoreactivity with αpMKS indicates the phosphorylation of YFP-DLP1 in cells (*lane 2*). Phosphorylation of endogenous DLP1 was barely visible (*lane 2*). Phosphatase treatment removed the αpMKS signal from the YFP-DLP1 (*lane 4*), and adding ERK1 re-phosphorylated the YFP-DLP1 (*asterisk, lane 6*). The lower band in the ERK1-treated sample (*lane 6*) is a nonspecific one. (**H**) The same experiment as in G using wild type (WT) and S616A mutant of YFP-DLP1. Immunoblotting with αpMKS shows that ERK1 phosphorylates wild-type YFP-DLP1 (*asterisk*) but not the S616 mutant. (For interpretation of the references to color in this figure legend, the reader is referred to the web version of this article at www.liebertonline.com/ars).

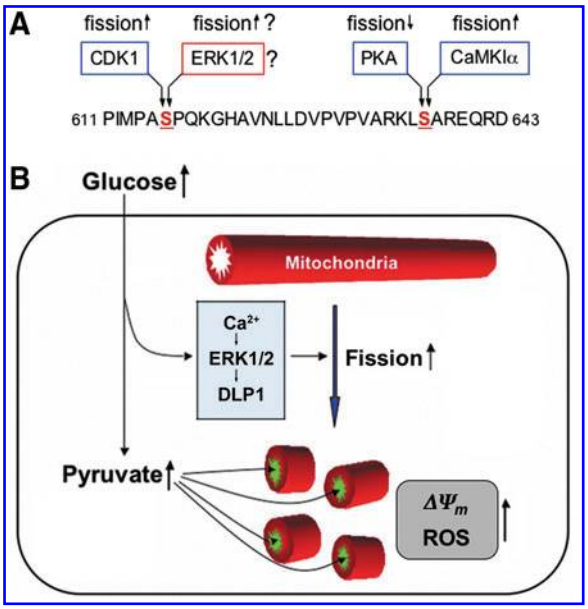

FIG. 9. High-glucose-induced signaling that increases mitochondrial fission and the ROS level. (**A**) Sites for DLP1 phosphorylation. Two serine residues (S616 and S637) of DLP1 are phosphorylated by cyclic AMP-dependent protein kinase (PKA), CamKIα, and cyclin-dependent kinase (CDK1). Dephosphorylation at the S637 is mediated by calcineurin. Details in the text. (**B**) The high-glucose concentration evokes cytosolic Ca^{2+} that activates ERK1/2. Active ERK1/2 potentially phosphorylates DLP1, promoting mitochondrial fragmentation *via* an increased mitochondrial association of DLP1. Mitochondrial fragmentation may facilitate the pyruvate uptake and/or affect the electron transport chain activity, resulting in the mitochondrial hyperpolarization and ROS overproduction. (For interpretation of the references to color in this figure legend, the reader is referred to the web version of this article at www.liebertonline.com/ars).

phosphorylated by CDK1 (Fig. 9A). Indeed, our experiments using the S616A mutant indicate that ERK1/2 phosphorylates DLP1 at this site (Fig. 8H).

As we reported previously (48), the acute exposure to high-glucose conditions induced a transient increase of mitochondrial fragmentation and ROS levels. In the current study, we observed a transient activation of ERK1/2 following the early Ca^{2+} signal. It is likely that, upon high-glucose stimulation, the increase and decrease of intracellular Ca^{2+} at the very upstream define the transient nature of all subsequent events in a time-delayed fashion. However, it is unclear what governs the transient nature of overall signaling that regulates mitochondrial morphology in high-glucose stimulation. Regarding the transient fragmentation of mitochondria, there may be an additional signaling that mediates the recovery of mitochondrial tubules. Maintaining normal mitochondrial morphology is important for proper cellular physiology. Possibly, cells sense the initial fragmentation of mitochondria and activate a recovery signal to prevent the harmful effect of mitochondrial fragmentation. If the ERK1/2-mediated DLP1 phosphorylation increases mitochondrial fission in high-glucose stimulation as suggested in this study, the recovery signal could involve dephosphorylation of DLP1at S616. While the Ca^{2+}-dependent phosphatase calcineurin dephosphorylates DLP1 at the cyclic AMP-dependent protein kinase-phosphorylated site (S637) (9, 16), the phosphatase dephosphorylating DLP1 at S616 is unknown. Additionally, ubiquitylation-mediated degradation of mitochondrial fission protein has been reported (32, 44). Degradation of fission proteins would counteract the fission activation by high-glucose stimulation. Transient mitochondrial fragmentation was also observed upon treating cells with thapsigargin that increases cytosolic Ca^{2+} (24). During the recovery of tubular mitochondria in thapsigargin incubation, mitochondrial tubules become excessively long, suggesting a possible overshoot by a compensatory recovery signaling (24). Similar to this, elongated mitochondria were frequently observed during recovery from mitochondrial fragmentation in high-glucose stimulation (results not shown).

Our preliminary experiments suggested a potential involvement of phosphatidylinositol 3-kinase (PI3K) in mitochondrial fragmentation in the high-glucose insult (results not shown). Interestingly, glycogen synthase kinase-3β, a downstream component of the PI3K pathway, has been reported to interact with and potentially phosphorylate DLP1 (12, 25). Cellular signaling pathways are intricately intertwined through complex crosstalk. It is of interest to find out whether ERK1/2 and PI3K operate in a linear or parallel pathway to activate mitochondrial fission. Our study presented here identified the early signaling pathway activated upon the acute high-glucose stimulation. We found that Ca^{2+} and ERK1/2 are the upstream components activating mitochondrial fission and ROS production (Fig. 9). Given the pathological role of mitochondrial fragmentation and ROS overproduction in hyperglycemia, further delineation of the signaling pathway that regulates mitochondrial fission in hyperglycemia will expand potential therapeutic targets for hyperglycemic and diabetic complications.

Acknowledgments

The authors would like to thank Chad Galloway for critical reading, and Li Wang and Jessica Sheu for technical assistance. The authors thank Luca Scorrano for providing YFP-fused DLP1 constructs. This study was supported by NIH grants DK078618 and DK061991 to Y.Y.

Author Disclosure Statement

No competing financial interests exist.

References

1. Alexander C, Votruba M, Pesch UE, Thiselton DL, Mayer S, Moore A, Rodriguez M, Kellner U, Leo-Kottler B, Auburger G, *et al.* OPA1, encoding a dynamin-related GTPase, is mutated in autosomal dominant optic atrophy linked to chromosome 3q28. *Nat Genet* 26: 211–215, 2000.
2. Allen DA, Yaqoob MM, and Harwood SM. Mechanisms of high glucose-induced apoptosis and its relationship to diabetic complications. *J Nutr Biochem* 16: 705–713, 2005.
3. Arnette D, Gibson TB, Lawrence MC, January B, Khoo S, McGlynn K, Vanderbilt CA, and Cobb MH. Regulation of ERK1 and ERK2 by glucose and peptide hormones in pancreatic beta cells. *J Biol Chem* 278: 32517–32525, 2003.

4. Berridge MJ, Bootman MD, and Roderick HL. Calcium signalling: dynamics, homeostasis and remodelling. *Nat Rev Mol Cell Biol* 4: 517–529, 2003.
5. Breckenridge DG, Stojanovic M, Marcellus RC, and Shore GC. Caspase cleavage product of BAP31 induces mitochondrial fission through endoplasmic reticulum calcium signals, enhancing cytochrome c release to the cytosol. *J Cell Biol* 160: 1115–1127, 2003.
6. Brownlee M. Biochemistry and molecular cell biology of diabetic complications. *Nature* 414: 813–820, 2001.
7. Cai L, Li W, Wang G, Guo L, Jiang Y, and Kang YJ. Hyperglycemia-induced apoptosis in mouse myocardium: mitochondrial cytochrome c-mediated caspase-3 activation pathway. *Diabetes* 51: 1938–1948, 2002.
8. Cave AC, Brewer AC, Narayanapanicker A, Ray R, Grieve DJ, Walker S, and Shah AM. NADPH oxidases in cardiovascular health and disease. *Antioxid Redox Signal* 8: 691–728, 2006.
9. Cereghetti GM, Stangherlin A, Martins de Brito O, Chang CR, Blackstone C, Bernardi P, and Scorrano L. Dephosphorylation by calcineurin regulates translocation of Drp1 to mitochondria. *Proc Natl Acad Sci U S A* 105: 15803–15808, 2008.
10. Chan DC. Mitochondria: dynamic organelles in disease, aging, and development. *Cell* 125: 1241–1252, 2006.
11. Chang CR and Blackstone C. Cyclic AMP-dependent protein kinase phosphorylation of Drp1 regulates its GTPase activity and mitochondrial morphology. *J Biol Chem* 282: 21583–21587, 2007.
12. Chen CH, Hwang SL, Howng SL, Chou CK, and Hong YR. Three rat brain alternative splicing dynamin-like protein variants: interaction with the glycogen synthase kinase 3beta and action as a substrate. *Biochem Biophys Res Commun* 268: 893–898, 2000.
13. Chen H and Chan DC. Mitochondrial dynamics—fusion, fission, movement, and mitophagy—in neurodegenerative diseases. *Hum Mol Genet* 18: R169–R176, 2009.
14. Chen H, Detmer SA, Ewald AJ, Griffin EE, Fraser SE, and Chan DC. Mitofusins Mfn1 and Mfn2 coordinately regulate mitochondrial fusion and are essential for embryonic development. *J Cell Biol* 160: 189–200, 2003.
15. Cipolat S, Martins de Brito O, Dal Zilio B, and Scorrano L. OPA1 requires mitofusin 1 to promote mitochondrial fusion. *Proc Natl Acad Sci U S A* 101: 15927–15932, 2004.
16. Cribbs JT and Strack S. Reversible phosphorylation of Drp1 by cyclic AMP-dependent protein kinase and calcineurin regulates mitochondrial fission and cell death. *EMBO Rep* 8: 939–944, 2007.
17. Delettre C, Lenaers G, Griffoin JM, Gigarel N, Lorenzo C, Belenguer P, Pelloquin L, Grosgeorge J, Turc-Carel C, Perret E, *et al.* Nuclear gene OPA1, encoding a mitochondrial dynamin-related protein, is mutated in dominant optic atrophy. *Nat Genet* 26: 207–210, 2000.
18. Detaille D, Guigas B, Chauvin C, Batandier C, Fontaine E, Wiernsperger N, and Leverve X. Metformin prevents high-glucose-induced endothelial cell death through a mitochondrial permeability transition-dependent process. *Diabetes* 54: 2179–2187, 2005.
19. Dorbani L, Jancsik V, Linden M, Leterrier JF, Nelson BD, and Rendon A. Subfractionation of the outer membrane of rat brain mitochondria: evidence for the existence of a domain containing the porin-hexokinase complex. *Arch Biochem Biophys* 252: 188–196, 1987.
20. Frodin M, Sekine N, Roche E, Filloux C, Prentki M, Wollheim CB, and Van Obberghen E. Glucose, other secretagogues, and nerve growth factor stimulate mitogen-activated protein kinase in the insulin-secreting beta-cell line, INS-1. *J Biol Chem* 270: 7882–7889, 1995.
21. Germain M, Mathai JP, McBride HM, and Shore GC. Endoplasmic reticulum BIK initiates DRP1-regulated remodelling of mitochondrial cristae during apoptosis. *EMBO J* 24: 1546–1556, 2005.
22. Han XJ, Lu YF, Li SA, Kaitsuka T, Sato Y, Tomizawa K, Nairn AC, Takei K, Matsui H, and Matsushita M. CaM kinase I alpha-induced phosphorylation of Drp1 regulates mitochondrial morphology. *J Cell Biol* 182: 573–585, 2008.
23. Hellman B, Gylfe E, Grapengiesser E, Lund PE, and Berts A. Cytoplasmic Ca2 + oscillations in pancreatic beta-cells. *Biochim Biophys Acta* 1113: 295–305, 1992.
24. Hom JR, Gewandter JS, Michael L, Sheu SS, and Yoon Y. Thapsigargin induces biphasic fragmentation of mitochondria through calcium-mediated mitochondrial fission and apoptosis. *J Cell Physiol* 212: 498–508, 2007.
25. Hong YR, Chen CH, Cheng DS, Howng SL, and Chow CC. Human dynamin-like protein interacts with the glycogen synthase kinase 3beta. *Biochem Biophys Res Commun* 249: 697–703, 1998.
26. Khoo S and Cobb MH. Activation of mitogen-activating protein kinase by glucose is not required for insulin secretion. *Proc Natl Acad Sci U S A* 94: 5599–5604, 1997.
27. Knott AB, Perkins G, Schwarzenbacher R, and Bossy-Wetzel E. Mitochondrial fragmentation in neurodegeneration. *Nat Rev Neurosci* 9: 505–518, 2008.
28. Kodali RB, Kim WJ, Galaria II, Miller C, Schecter AD, Lira SA, and Taubman MB. CCL11 (Eotaxin) induces CCR3-dependent smooth muscle cell migration. *Arterioscler Thromb Vasc Biol* 24: 1211–1216, 2004.
29. Koopman WJ, Verkaart S, Visch HJ, van der Westhuizen FH, Murphy MP, van den Heuvel LW, Smeitink JA, and Willems PH. Inhibition of complex I of the electron transport chain causes $O2^{-}$-mediated mitochondrial outgrowth. *Am J Physiol Cell Physiol* 288: C1440–C1450, 2005.
30. Koshiba T, Detmer SA, Kaiser JT, Chen H, McCaffery JM, and Chan DC. Structural basis of mitochondrial tethering by mitofusin complexes. *Science* 305: 858–862, 2004.
31. Kurokawa M, Kimura J, Tokuoka S, and Ishibashi S. Binding potential of brain hexokinase to mitochondria membrane. *Brain Res* 175: 169–173, 1979.
32. Nakamura N, Kimura Y, Tokuda M, Honda S, and Hirose S. MARCH-V is a novel mitofusin 2- and Drp1-binding protein able to change mitochondrial morphology. *EMBO Rep* 7: 1019–1022, 2006.
33. Nishikawa T, Edelstein D, Du XL, Yamagishi S, Matsumura T, Kaneda Y, Yorek MA, Beebe D, Oates PJ, Hammes HP, *et al.* Normalizing mitochondrial superoxide production blocks three pathways of hyperglycaemic damage. *Nature* 404: 787–790, 2000.
34. Parry DM and Pedersen PL. Intracellular localization of rat kidney hexokinase. Evidence for an association with low density mitochondria. *J Biol Chem* 259: 8917–8923, 1984.
35. Pitts KR, Yoon Y, Krueger EW, and McNiven MA. The dynamin-like protein DLP1 is essential for normal distribution and morphology of the endoplasmic reticulum and mitochondria in mammalian cells. *Mol Biol Cell* 10: 4403–4417, 1999.
36. Russell JW, Golovoy D, Vincent AM, Mahendru P, Olzmann JA, Mentzer A, and Feldman EL. High glucose-induced oxidative stress and mitochondrial dysfunction in neurons. *FASEB J* 16: 1738–1748, 2002.

37. Smirnova E, Griparic L, Shurland DL, and van der Bliek AM. Dynamin-related protein Drp1 is required for mitochondrial division in mammalian cells. *Mol Biol Cell* 12: 2245–2256, 2001.
38. Soejima A, Inoue K, Takai D, Kaneko M, Ishihara H, Oka Y, and Hayashi JI. Mitochondrial DNA is required for regulation of glucose-stimulated insulin secretion in a mouse pancreatic beta cell line, MIN6. *J Biol Chem* 271: 26194–26199, 1996.
39. Szabadkai G, Simoni AM, Bianchi K, De Stefani D, Leo S, Wieckowski MR, and Rizzuto R. Mitochondrial dynamics and Ca2+ signaling. *Biochim Biophys Acta* 1763: 442–449, 2006.
40. Taguchi N, Ishihara N, Jofuku A, Oka T, and Mihara K. Mitotic phosphorylation of dynamin-related GTPase Drp1 participates in mitochondrial fission. *J Biol Chem* 282: 11521–11529, 2007.
41. Tamareille S, Mignen O, Capiod T, Rucker-Martin C, and Feuvray D. High glucose-induced apoptosis through store-operated calcium entry and calcineurin in human umbilical vein endothelial cells. *Cell Calcium* 39: 47–55, 2006.
42. Theler JM, Mollard P, Guerineau N, Vacher P, Pralong WF, Schlegel W, and Wollheim CB. Video imaging of cytosolic Ca2+ in pancreatic beta-cells stimulated by glucose, carbachol, and ATP. *J Biol Chem* 267: 18110–18117, 1992.
43. Wilson JE. The localization of latent brain hexokinase on synaptosomal mitochondria. *Arch Biochem Biophys* 150: 96–104, 1972.
44. Yonashiro R, Ishido S, Kyo S, Fukuda T, Goto E, Matsuki Y, Ohmura-Hoshino M, Sada K, Hotta H, Yamamura H, *et al.* A novel mitochondrial ubiquitin ligase plays a critical role in mitochondrial dynamics. *EMBO J* 25: 3618–3626, 2006.
45. Yoon Y, Krueger EW, Oswald BJ, and McNiven MA. The mitochondrial protein hFis1 regulates mitochondrial fission in mammalian cells through an interaction with the dynamin-like protein DLP1. *Mol Cell Biol* 23: 5409–5420, 2003.
46. Yoon Y, Pitts KR, Dahan S, and McNiven MA. A novel dynamin-like protein associates with cytoplasmic vesicles and tubules of the endoplasmic reticulum in mammalian cells. *J Cell Biol* 140: 779–793, 1998.
47. Yoon Y, Pitts KR, and McNiven MA. Mammalian dynamin-like protein DLP1 tubulates membranes. *Mol Biol Cell* 12: 2894–2905, 2001.
48. Yu T, Robotham JL, and Yoon Y. Increased production of reactive oxygen species in hyperglycemic conditions requires dynamic change of mitochondrial morphology. *Proc Natl Acad Sci U S A* 103: 2653–2658, 2006.
49. Yu T, Sheu SS, Robotham JL, and Yoon Y. Mitochondrial fission mediates high glucose-induced cell death through elevated production of reactive oxygen species. *Cardiovasc Res* 79: 341–351, 2008.
50. Zuchner S, Mersiyanova IV, Muglia M, Bissar-Tadmouri N, Rochelle J, Dadali EL, Zappia M, Nelis E, Patitucci A, Senderek J, *et al.* Mutations in the mitochondrial GTPase mitofusin 2 cause Charcot-Marie-Tooth neuropathy type 2A. *Nat Genet* 36: 449–451, 2004.

Address correspondence to:
Prof. Yisang Yoon
Department of Anesthesiology
University of Rochester School of Medicine and Dentistry
601 Elmwood Ave., Box 604
Rochester, NY 14642

E-mail: yisang_yoon@urmc.rochester.edu

Date of first submission to ARS Central, May 7, 2010; date of acceptance, June 2, 2010.

Abbreviations Used

AR = aspect ratio
CDK1 = cyclin-dependent kinase 1
DHE = dihydroethidium
DLP1 = dynamin-like protein 1
DMEM = Dulbecco's modified Eagle's medium
EGTA = ethylene glycol bis(2-aminoethyl ether)-*N*,*N*,*N*′,*N*′-tetraacetic acid
ERK1/2 = extracellular signal-regulated kinase 1/2
ETC = electron transport chain
FBS = fetal bovine serum
FF = form factor
MAP = mitogen-activated protein
PI3K = phosphatidylinositol 3-kinase
PKA = cyclic AMP-dependent protein kinase
ROS = reactive oxygen species
SMC = smooth muscle cell
VDAC = voltage-dependent anion channel
YFP = yellow fluorescent protein

This article has been cited by:

1. Ya-Xing Gui, Xin-Yi Wang, Wen-Yan Kang, Ying-Jie Zhang, Yu Zhang, Yong Zhou, Thomas J. Quinn, Jun Liu, Sheng-Di Chen. 2012. Extracellular signal-regulated kinase is involved in alpha-synuclein-induced mitochondrial dynamic disorders by regulating dynamin-like protein 1. *Neurobiology of Aging* **33**:12, 2841-2854. [CrossRef]
2. Chad A. Galloway, Hakjoo Lee, Yisang Yoon. 2012. Mitochondrial morphology – Emerging role in bioenergetics. *Free Radical Biology and Medicine* . [CrossRef]
3. Chad A. Galloway , Yisang Yoon . Mitochondrial Morphology in Metabolic Diseases. *Antioxidants & Redox Signaling*, ahead of print. [Abstract] [Full Text HTML] [Full Text PDF] [Full Text PDF with Links]
4. María Morán, David Moreno-Lastres, Lorena Marín-Buera, Joaquín Arenas, Miguel A. Martín, Cristina Ugalde. 2012. Mitochondrial respiratory chain dysfunction: Implications in neurodegeneration. *Free Radical Biology and Medicine* **53**:3, 595-609. [CrossRef]
5. Felix Distelmaier , Federica Valsecchi , Marleen Forkink , Sjenet van Emst-de Vries , Herman G. Swarts , Richard J.T. Rodenburg , Eugène T.P. Verwiel , Jan A.M. Smeitink , Peter H.G.M. Willems , Werner J.H. Koopman . Trolox-Sensitive Reactive Oxygen Species Regulate Mitochondrial Morphology, Oxidative Phosphorylation and Cytosolic Calcium Handling in Healthy Cells. *Antioxidants & Redox Signaling*, ahead of print. [Abstract] [Full Text HTML] [Full Text PDF] [Full Text PDF with Links] [Supplemental material]
6. C. A. Galloway, Y. Yoon. 2012. Perspectives on: SGP Symposium on Mitochondrial Physiology and Medicine: What comes first, misshape or dysfunction? The view from metabolic excess. *The Journal of General Physiology* **139**:6, 455-463. [CrossRef]
7. Marilyn J. Hammer, Joachim G. Voss. 2012. Malglycemia and Cancer: Introduction to a Conceptual Model. *Oncology Nursing Forum* **39**:3, E275-E287. [CrossRef]
8. Hongshan Ge, Theodore L. Tollner, Zhen Hu, Mimi Da, Xiaohe Li, HeQin Guan, Dan Shan, Jieqiang Lu, Changjiang Huang, Qiaoxiang Dong. 2012. Impaired mitochondrial function in murine oocytes is associated with controlled ovarian hyperstimulationand in vitro maturation. *Reproduction, Fertility and Development* **24**:7, 945. [CrossRef]
9. Jian Yang, Yu Han, Hailan Sun, Caiyu Chen, Duofen He, Jing Guo, Changqing Yu, Baoquan Jiang, Lin Zhou, Chunyu Zeng. 2011. (-)-Epigallocatechin Gallate Suppresses Proliferation of Vascular Smooth Muscle Cells Induced by High Glucose by Inhibition of PKC and ERK1/2 Signalings. *Journal of Agricultural and Food Chemistry* 111014104727005. [CrossRef]
10. Shinko Kobashigawa, Keiji Suzuki, Shunichi Yamashita. 2011. Ionizing radiation accelerates Drp1-dependent mitochondrial fission, which involves delayed mitochondrial reactive oxygen species production in normal human fibroblast-like cells. *Biochemical and Biophysical Research Communications* . [CrossRef]